BIOCHEMISTRY
including biophysical chemistry & molecular biology

Article

pubs.acs.org/biochemistry

Crystal Structure and Thermodynamic and Kinetic Stability of Metagenome-Derived LC-Cutinase

Sintawee Sulaiman,[†] Dong-Ju You,[†,‡] Eiko Kanaya,[†] Yuichi Koga,[†] and Shigenori Kanaya*[,†]

[†]Department of Material and Life Science, Graduate School of Engineering, Osaka University, 2-1 Yamadaoka, Suita, Osaka 565-0871, Japan

[‡]Division of Electron Microscopic Research, Korea Basic Science Institute (KBSI), 113 Gwahangno, Yuseong-gu, Daejeon 305-333, Korea

Supporting Information

ABSTRACT: The crystal structure of metagenome-derived LC-cutinase with polyethylene terephthalate (PET)-degrading activity was determined at 1.5 Å resolution. The structure strongly resembles that of *Thermobifida alba* cutinase. Ser165, Asp210, and His242 form the catalytic triad. Thermal denaturation and guanidine hydrochloride (GdnHCl)-induced unfolding of LC-cutinase were analyzed at pH 8.0 by circular dichroism spectroscopy. The midpoint of the transition of the thermal denaturation curve, $T_{1/2}$, and that of the GdnHCl-induced unfolding curve, C_m, at 30 °C were 86.2 °C and 4.02 M, respectively. The free energy change of unfolding in the absence of GdnHCl, $\Delta G(H_2O)$, was 41.8 kJ mol^{-1} at 30 °C. LC-cutinase unfolded very slowly in GdnHCl with an unfolding rate, $k_u(H_2O)$, of 3.28 × 10^{-6} s^{-1} at 50 °C. These results indicate that LC-cutinase is a kinetically robust protein. Nevertheless, the optimal temperature for the activity of LC-cutinase toward *p*-nitrophenyl butyrate (50 °C) was considerably lower than the $T_{1/2}$ value. It increased by 10 °C in the presence of 1% polyethylene glycol (PEG) 1000. It also increased by at least 20 °C when PET was used as a substrate. These results suggest that the active site is protected from a heat-induced local conformational change by binding of PEG or PET. LC-cutinase contains one disulfide bond between Cys275 and Cys292. To examine whether this disulfide bond contributes to the thermodynamic and kinetic stability of LC-cutinase, C275/292A-cutinase without this disulfide bond was constructed. Thermal denaturation studies and equilibrium and kinetic studies of the GdnHCl-induced unfolding of C275/292A-cutinase indicate that this disulfide bond contributes not only to the thermodynamic stability but also to the kinetic stability of LC-cutinase.

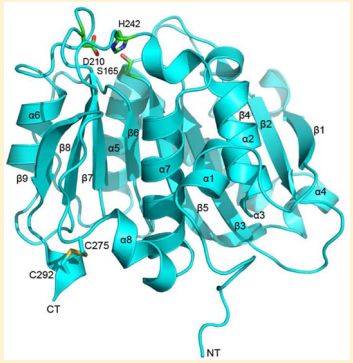

Cutinase is an enzyme that hydrolyzes cutin, which is a major component of plant cuticle.[1] It can also hydrolyze water-soluble esters, emulsified short- and long-chain triacylglycerols, and synthetic polyesters, such as poly(ε-caprolactone) (PCL) and polyethylene terephthalate (PET).[2−4] It does not undergo interfacial activation. Cutinase has been isolated from a variety of fungi, such as *Fusarium solani pisi*, *Aspergillus oryzae*, *Humilica insolens*, *Monilinia fructicola*, and *Pyrenopeziza brassicae*, several bacteria, such as *Thermobifida fusca* and *Thermobifida alba*, and yeast *Cryptococcus* sp. S-2.[5] The crystal structures of cutinases from *F. solani pisi*,[3] *Glomerella cingulata*,[6] *A. oryzae*,[7] *T. alba*,[8] and *Cryptococcus* sp. S-2[9] have been determined. According to these structures, cutinase has a typical α/β-hydrolase fold with the catalytic triad consisting of Ser, His, and Asp. It does not have a lid structure, which is responsible for interfacial activation of lipase. Because of its ability to hydrolyze a wide range of ester bonds and to catalyze the esterification and transesterification reactions, cutinase has been thought to be a promising enzyme for industrial uses in a variety of fields, such as the textile industry, detergent manufacturing, food processing, polymer chemistry, PET recycling, and biofuel production.[2−5,10] To meet the requirement of industrial applications, attempts to improve the enzymatic properties, mainly activity, of cutinase have been made.[7,11−16] However, to engineer a cutinase variant with higher activity and stability in a rational manner, a thorough understanding of the structure−activity−stability relationships of cutinase is necessary.

LC-cutinase is a cutinase homologue isolated from leaf-branch compost by using a metagenomic approach.[17] The source organism of this enzyme remains to be identified. However, it is presumably a thermophilic bacterium, because the temperature of the compost from which this enzyme is isolated is 67 °C and LC-cutinase shows higher degrees of amino acid sequence similarity to thermophilic bacterial cutinases than to fungal cutinases. For example, the amino acid sequence of LC-cutinase is 56.8% identical to that of *T. fusca* cutinase and 14.9% identical to that of *F. solani pisi* cutinase, which represent bacterial and fungal cutinases, respectively. LC-cutinase is a secretory protein and consists of 258 amino acid residues (molecular mass of 28 kDa). It is overproduced in *Escherichia coli* as a fusion protein with the

Received: November 21, 2013
Revised: March 3, 2014
Published: March 4, 2014

pelB leader sequence and is purified from the extracellular medium in a form with a piece of the pelB leader sequence at the N-terminus. LC-cutinase is monomeric and hydrolyzes various fatty acid monoesters most optimally at pH 8.5 and 50 °C. It also effectively hydrolyzes PCL and PET. Thus, LC-cutinase serves as a good model for analyzing the structure−activity−stability relationships of cutinase. However, its crystal structure remains to be determined. Its thermodynamic and kinetic stability also remains to be analyzed.

The melting temperatures, T_m, of *F. solani pisi* and *A. oryzae* cutinases have been reported to be 56 and 59 °C, respectively.[7] The free energy changes of unfolding in the absence of GdnHCl, $\Delta G(H_2O)$, of *F. solani pisi* and *H. insolens* cutinases have been reported to be 47.0 and 49.4 kJ mol^{-1}, respectively.[18] The unfolding rates, $k_u(H_2O)$, of *F. solani pisi* and *H. insolens* cutinases have been reported to be 2.57 and 0.83 s^{-1}, respectively.[18] However, none of the parameters characterizing thermal denaturation and GdnHCl-induced unfolding of bacterial cutinases has been reported.

In this study, we determined the crystal structure of LC-cutinase and analyzed its stability. We showed that the structure of LC-cutinase strongly resembles that of *T. alba* cutinase and contains one disulfide bond between Cys275 and Cys292. We also showed that LC-cutinase is a kinetically robust protein. The temperature dependence of the activity of LC-cutinase in the presence of PEG or that toward PET suggests that the conformation of the active site is locally changed before the protein is thermally denatured and the active site is protected from this conformational change by binding of PEG or PET. Construction of the LC-cutinase derivative (C275/292A-cutinase) without the disulfide bond, followed by the analyses of its stability, indicates that this disulfide bond contributes to the thermodynamic and kinetic stability of LC-cutinase.

MATERIALS AND METHODS

Protein Preparation. The pET25b derivative for the overproduction of C275/292A-cutinase was constructed with the KOD plus mutagenesis kit (Toyobo, Osaka, Japan). The pET25b derivative for overproduction of the pelB-LC-cutinase[36−293] fusion protein[17] was used as a template. The primers for the polymerase chain reaction (PCR) were designed such that both TGC codons for Cys275 and Cys292 are changed to GCC for Ala. PCR was performed using a thermal cycler (Gene Amp PCR system 2400, Applied Biosystems, Tokyo, Japan). All DNA oligomers were synthesized by Hokkaido System Science (Sapporo, Japan). The nucleotide sequence was confirmed with a Prism 3100 DNA sequencer (Applied Biosystems).

LC- and C275/292A-cutinases were overproduced in *E. coli* BL21-CodonPlus (DE3)-RP as a fusion protein with the pelB leader sequence and purified from the extracellular medium, as described previously.[17] The protein concentration was determined from the UV absorption on the basis that the absorbance of a 0.1% (1.0 mg mL^{-1}) solution at 280 nm is 1.37. This value was calculated by using ε values of 1526 M^{-1} cm^{-1} for tyrosine and 5225 M^{-1} cm^{-1} for tryptophan at 280 nm.[19]

Crystallization and Structure Determination. Crystallization of LC-cutinase was conducted at 20 °C using a sitting drop vapor diffusion method in a 96-well Corning Crystal*EX* plate (Hampton Research, Aliso Viejo, CA). Drop solutions were prepared by mixing 1 μL each of protein and reservoir solutions and equilibrated against a 100 μL reservoir solution. LC-cutinase was concentrated to approximately 11 mg mL^{-1} before crystallization. The crystallization conditions were screened using Wizard III and IV (Emerald BioStructures, Inc. & Emerald BioSystems, Bainbridge Island, WA). Crystals of LC-cutinase appeared in the drops containing 20% (w/v) polyethylene glycol (PEG) 3350 and 0.2 M sodium thiocyanate after incubation for 2 weeks. These crystals belonged to space group $P2_12_12_1$, contained one protein molecule per asymmetric unit, and had the following cell parameters: a = 40.91 Å, b = 71.08 Å, and c = 72.73 Å.

Diffraction data of LC-cutinase were collected at a wavelength of 0.9 Å on beamline BL44XU at SPring-8. The data were indexed, integrated, and scaled using the HKL2000 program suite.[20] The structure was determined by the molecular replacement method using MOLREP[21] in the CCP4 program suite.[22] The crystal structure of *Streptomyces exfoliatus* lipase at 1.9 Å resolution was used as a starting model. Automated model building was conducted using ArpWarp.[23] Structural refinement was conducted by using REFMAC[24] of the CCP4 program, and the model was corrected using COOT.[25] The statistics for data collection and refinement are summarized in Table 1. The coordinates and structure factors have been deposited in the Protein Data Bank (PDB) as entry 4EB0.

Table 1. Data Collection and Refinement Statistics of LC-Cutinase

Data Collection	
wavelength (Å)	0.9
space group	$P2_12_12_1$
cell parameters	
a, b, c (Å)	40.91, 71.08, 72.73
$\alpha = \beta = \gamma$ (deg)	90.0
no. of molecules per asymmetric unit	1
resolution range (Å)	50.0−1.5 (1.53−1.5)[a]
no. of reflections measured	480881
no. of unique reflections	35110
completeness (%)	99.9 (100)[a]
R_{merge} (%)[b]	10.6 (41.9)[a]
average $I/\sigma(I)$	31.7 (4.1)[a]
Refinement	
resolution limits (Å)	50.0−1.5
no. of atoms	
protein	1962
water	315
SCN	12
R_{work} (%)/R_{free} (%)[c]	15.7/18.6
rmsd from ideal values	
bond lengths (Å)	0.007
bond angles (deg)	1.00
average B factor (Å^2)	
protein	15.5
water	27.1
SCN	23.6
Ramachandran plot statistics	
most favored regions (%)	97.3
additional allowed regions (%)	2.7

[a]Numbers in parentheses are for the highest-resolution shell. [b]$R_{merge} = \sum|I_{hkl} - \langle I_{hkl}\rangle|/\sum I_{hkl}$, where I_{hkl} is an intensity measurement for a reflection with indices hkl and $\langle I_{hkl}\rangle$ is the mean intensity for multiply recorded reflections. [c]R_{free} was calculated using 5% of the total reflections chosen randomly and omitted from refinement.

dx.doi.org/10.1021/bi401561p | *Biochemistry* 2014, 53, 1858−1869

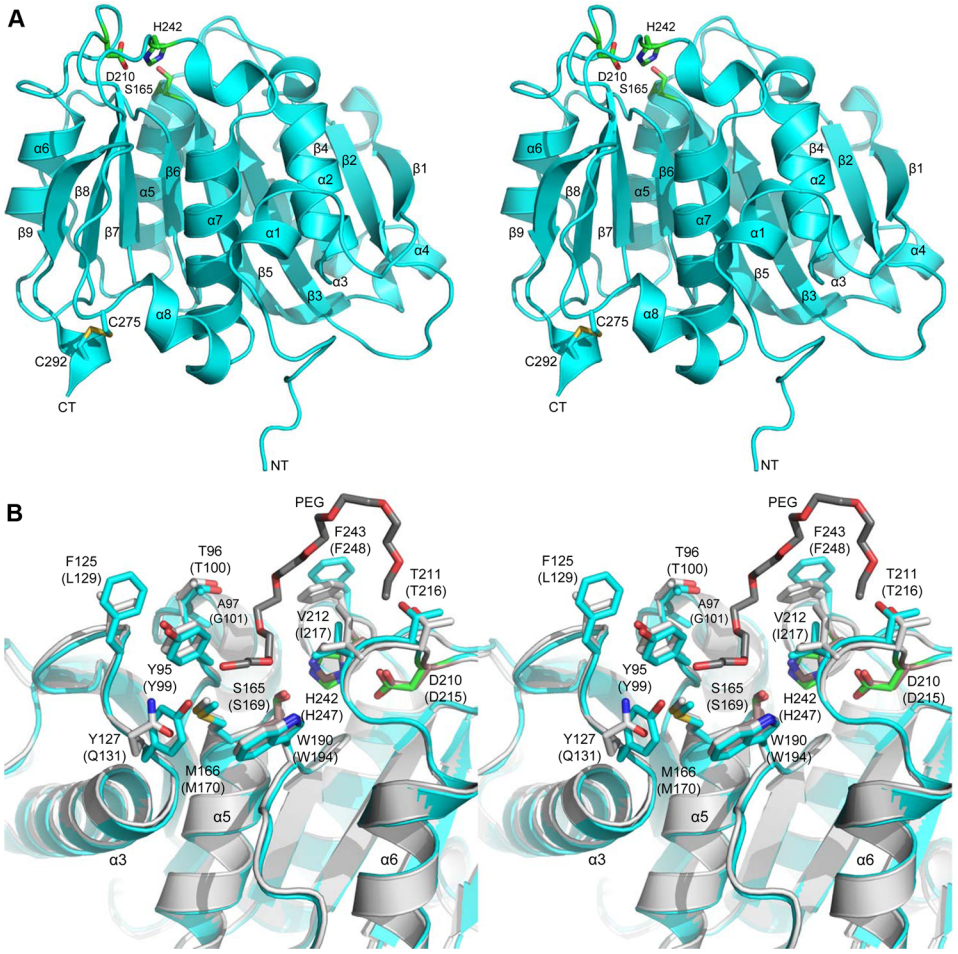

Figure 1. Stereoview of the crystal structure of LC-cutinase. (A) The entire structure of LC-cutinase is shown. Three active site residues (Ser165, Asp210, and His242) are shown as green stick models, in which the oxygen and nitrogen atoms are colored red and blue, respectively. The disulfide bond formed between Cys275 and Cys292 is also shown as a stick model, in which the sulfur atom is colored yellow. NT and CT represent the N- and C-termini, respectively. (B) The structure of LC-cutinase around the active site is superimposed on that of *T. alba* cutinase (PDB entry 3VIS chain A). The structures of LC-cutinase and *T. alba* cutinase are colored cyan and gray, respectively. The residues that form a hydrophobic patch on the protein surface and three active site residues of LC-cutinase are shown as stick models (green ones for active site residues) with labels. The corresponding residues of *T. alba* cutinase are also shown as stick models with labels in parentheses. In these stick models, the oxygen and nitrogen atoms are colored red and blue, respectively. A part of the PEG molecule bound to *T. alba* cutinase is indicated by a dark gray stick model, in which the oxygen atom is colored red.

Circular Dichroism (CD) Spectroscopy. The far-UV (200−260 nm) and near-UV (250−320 nm) CD spectra of the protein were measured on a J-725 spectropolarimeter (Japan Spectroscopic Co., Tokyo, Japan) at 20 °C. The protein was dissolved in 10 mM Tris-HCl (pH 8.0). The protein concentration and optical path length were 0.1 mg mL^{-1} and 2 mm for far-UV CD spectra and 1.0 mg mL^{-1} and 1 cm for near-UV CD spectra, respectively. The mean residue ellipticity, $[\theta]$, which has the units of degrees square centimeters per decimole, was calculated by using an average amino acid molecular mass of 110 Da.

Thermal Denaturation. Thermal denaturation curves of the proteins were obtained by monitoring the change in CD values at 222 nm as the temperature was increased. The proteins were dissolved in 10 mM sodium phosphate (pH 8.0) or the same buffer containing 10 mM dithiothreitol (DTT), 10 mM $CaCl_2$, or 1% PEG 1000. The protein concentration and optical path length were 0.1 mg mL^{-1} and 2 mm, respectively. The rate of temperature increase was 1.0 °C min^{-1}. The temperature of the midpoint of the transition, $T_{1/2}$, was calculated by curve fitting of the resultant CD values versus temperature data on the basis of a least-squares analysis.

Equilibrium Experiments for GdnHCl-Induced Unfolding. GdnHCl-induced unfolding of the protein was analyzed by monitoring the change in CD values at 222 nm, as described previously.[26] The protein concentration and optical path length were 0.1 mg mL^{-1} and 2 mm, respectively. The protein was incubated in 10 mM Tris-HCl (pH 8.0) containing various concentrations of guanidine hydrochloride (GdnHCl) at 30 °C for 48 h for LC-cutinase and 24 h for C275/292A-cutinase prior to the measurement of the CD values. The GdnHCl-induced unfolding curves were determined, and the nonlinear least-squares analysis[27] was used to fit the data to

$$y = \frac{b_n^0 + a_n[D] + (b_u^0 + a_u[D])\exp\left(\frac{\Delta G(H_2O) - m[D]}{RT}\right)}{1 + \exp\left(\frac{\Delta G(H_2O) - m[D]}{RT}\right)} \quad (1)$$

$$C_m = \frac{\Delta G(H_2O)}{m} \quad (2)$$

dx.doi.org/10.1021/bi401561p | *Biochemistry* 2014, 53, 1858−1869

where y is the observed CD signal at a given concentration of GdnHCl, [D] is the concentration of GdnHCl, b_n^0 and b_u^0 are the CD signals for the native and unfolded states, respectively, a_n and a_u are the slopes of the pretransition and posttransition of the baseline, respectively, $\Delta G(H_2O)$ is the Gibbs energy change (ΔG) of unfolding in the absence of GdnHCl, m is the slope of the linear correlation between ΔG and the GdnHCl concentration, and C_m is the GdnHCl concentration at the midpoint of the curve. The raw experimental data were directly fit to eq 1 using SigmaPlot. Two replicates were measured for each condition.

Kinetic Experiments Examining GdnHCl-Induced Unfolding. The unfolding reactions of the proteins were performed at 50 °C in 10 mM Tris-HCl (pH 8.0) and followed by measurement of CD spectra at 222 nm, as described previously.[26] The unfolding reaction was initiated by mixing the protein solution and GdnHCl solution, such that the final protein and GdnHCl concentrations become 0.1 mg mL^{-1} and 5−6 M for LC-cutinase or 3−4 M for C275/292A-cutinase, respectively. The kinetic data were analyzed using eq 3:

$$A(t) - A(\infty) = \sum A_i e^{-k_i t} \quad (3)$$

where $A(t)$ is the value of the CD signal at a given time t, $A(\infty)$ is the value when no further change is observed, K_i is the apparent rate constant of the ith kinetic phase, and A_i is the amplitude of the ith phase. The GdnHCl concentration dependence of the logarithms of the apparent rate constant (k_{app}) for unfolding was also examined. The rate constant for unfolding in the absence of GdnHCl [$k_u(H_2O)$] was calculated by fitting to eq 4:

$$\ln k_{app} = \ln k_u(H_2O) + m_u[D] \quad (4)$$

where [D] is the concentration of GdnHCl and m_u is the slope of the linear correlation of ln k_u with the GdnHCl concentration.

Determination of Enzymatic Activity. The enzymatic activity was determined at the temperature indicated in 10 mM Tris-HCl (pH 8.0) containing 10% (v/v) acetonitrile and 0.5 or 2 mM p-nitrophenyl butyrate (pNP-butyrate), as described previously.[17] The amount of p-nitrophenol (pNP) released from the substrate was determined from the absorption at 412 nm with an absorption coefficient of 14200 M^{-1} cm^{-1} with an automatic spectrophotometer (model U2810 spectrophotometer, Hitachi High-Technologies, Tokyo, Japan). One unit of activity was defined as the amount of enzyme that produced 1 μmol of pNP/min. For determination of the kinetic parameters, the substrate concentration was varied from 0.05 to 5 mM. The enzymatic reaction followed Michaelis−Menten kinetics, and the kinetic parameters were determined from the Lineweaver−Burk plot.

Detection of PET-Degrading Activity. PET-degrading activity was determined by measuring the weight loss of a PET film, which was cut into a piece with values of length, width, and thickness of approximately 5, 5, and 0.6 mm, respectively (20−25 mg), after incubation with the enzyme in 100 mM Tris-HCl (pH 8.0) at the indicated temperature, as described previously.[17] A PET film used as packaging containers of home electronics, which was processed and molded from amorphous PET, was obtained from Sanwa Supply Co., Ltd. (Okayama, Japan).

RESULTS AND DISCUSSION

Crystal Structure of LC-Cutinase. The recombinant protein of LC-cutinase was purified from the extracellular medium of *E. coli* cells as QPAMAMD-LC-cutinase, in which a seven-residue peptide, Gln-Pro-Ala-Met-Ala-Met-Asp, is attached to the N-terminus of LC-cutinase[36−293], as reported previously.[17] This seven-residue peptide is mostly derived from the pelB leader sequence, and LC-cutinase[36−293] represents LC-cutinase without a putative N-terminal signal peptide (Met1−Ala34) and Gln35. This protein will be simply designated as LC-cutinase hereafter. LC-cutinase was screened for crystallization conditions using the kits available from commercial sources. Crystals suitable for X-ray crystallographic analyses were obtained in 2 weeks.

The crystal structure of LC-cutinase was determined at 1.5 Å resolution. The asymmetric unit of the crystal structure consists of one molecule. The protein contains 258 of 265 residues, with the seven N-terminal residues missing. Electron density for these residues is not observed, probably because of structural disorder. The LC-cutinase structure belongs to the α/β hydrolase fold superfamily and consists of a nine-stranded β-sheet and eight α-helices (Figure 1A). It closely resembles the structures of *T. alba* cutinase (PDB entry 3VIS)[28] and *S. exfoliatus* lipase (PDB entry 1JFR).[29] The rmsd between LC-cutinase and *T. alba* cutinase is 0.77 Å for 255 Cα atoms, and that between LC-cutinase and *S. exfoliatus* lipase is 1.01 Å for 252 Cα atoms. The LC-cutinase structure reveals that Ser165, Asp210, and His242 form a catalytic triad. Ser165 within a GXSXG motif (GHSMG for LC-cutinase and its homologues) is located within a sharp turn, termed the nucleophilic elbow,[30] between strand β5 and helix α5 (Figure S1 of the Supporting Information). It also reveals that one disulfide bond is formed between Cys275 and Cys292. This disulfide bond apparently anchors the C-terminus to the loop between helix α8 and strand β9 as does that of *T. alba* cutinase between Cys280 and Cys298 (Figure S1 of the Supporting Information).

The structure of LC-cutinase around the active site is compared with that of *T. alba* cutinase in Figure 1B. The *T. alba* cutinase structure shows that Tyr99, Thr100, Leu129, Met170, Trp194, Thr216, Ile217, and Phe248 form a hydrophobic patch on the protein surface, to which a polyethylene glycol (PEG) partially binds.[28] Three active site residues, Ser169, Asp215, and His247, are embedded in this hydrophobic patch. The corresponding residues of LC-cutinase are Tyr95, Thr96, Phe125, Met166, Trp190, Thr211, Val212, and Phe243. These residues, as well as Ala97 and Tyr127, which are replaced with Gly (Gly101) and Gln (Gln131), respectively, in *T. alba* cutinase, apparently form a hydrophobic patch. A long groove is extended from the catalytic pocket in this hydrophobic patch, suggesting that this groove serves as a binding site of an amphiphilic long-chain substrate, such as PET. However, further structural studies will be necessary to understand the substrate recognition mechanism of the enzyme.

Thermal Stability of LC-Cutinase. Thermal denaturation of LC-cutinase was analyzed at pH 8.0 by monitoring the change in CD values at 222 nm. This pH was chosen, because LC-cutinase exhibits nearly the highest activity at this pH.[17] Thermal denaturation of LC-cutinase was irreversible under the condition examined. However, the thermal denaturation curve of this protein was reproducible unless the protein concentration, the pH, and the rate of the temperature increase (scan

dx.doi.org/10.1021/bi401561p | *Biochemistry* 2014, 53, 1858−1869

rate) were significantly changed. The thermal denaturation curve of LC-cutinase measured in 10 mM phosphate buffer (pH 8.0) is shown in Figure 2. The midpoint of the transition

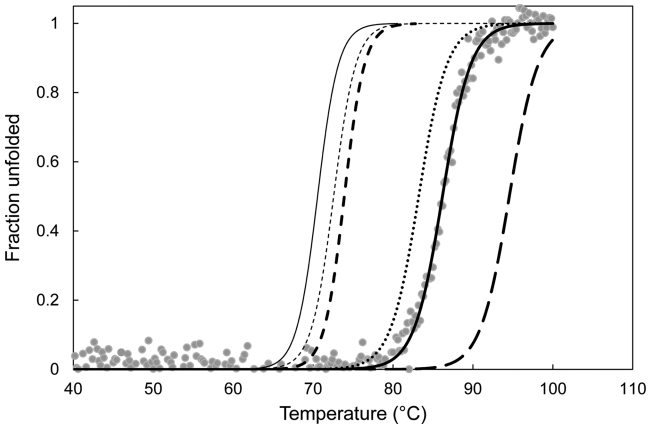

Figure 2. Thermal denaturation curves of LC-cutinase and C275/292A-cutinase. The thermal denaturation curves of LC-cutinase obtained in the absence of DTT (thick solid line), in the absence of DTT and presence of 10 mM $CaCl_2$ (thick long dashed line), in the absence of DTT and presence of 1% PEG (thick dotted line), and in the presence of 10 mM DTT (thick dashed line) and those of C275/292A-cutinase obtained in the absence of DTT (thin solid line) and in the presence of 10 mM DTT (thin dashed line) are shown. The rate of temperature increase was 1 °C/min. The lines represent optimal fits to the data, which are only shown for LC-cutinase in the absence of DTT as a representative (solid gray circles).

of this curve, $T_{1/2}$, was 86.2 °C (Table 2). This value is higher than the melting temperature (T_m) of *T. alba* cutinase, which has been determined to be 60 °C by differential scanning calorimetry,[31] by approximately 26 °C.

Table 2. $T_{1/2}$ Values of LC-Cutinase and C275/292A-Cutinase at pH 8.0

protein	[DTT] (mM)	[$CaCl_2$] (mM)	PEG (%)	$T_{1/2}$[a] (°C)	$\Delta T_{1/2}$[b] (°C)
LC-cutinase	0	0	0	86.2 ± 0.2	–
	10	0	0	73.9 ± 0.2	−12.3
	0	10	0	94.6 ± 0.4	+8.4
	0	0	1	83.2 ± 0.2	−3.0
C275/292A-cutinase	0	0	0	70.6 ± 0.1	−15.6
	10	0	0	72.6 ± 0.1	−13.6

[a]The denaturation temperature ($T_{1/2}$), which is the temperature of the midpoint of the transition, was determined from the thermal denaturation curves shown in Figure 2. [b]$\Delta T_{1/2}$ = $T_{1/2}$ determined − 86.2 °C.

The *T. alba* cutinase structure has been determined as a dimer in the presence of PEG.[28] PEG binds to the region near the active site, such that two monomers share one PEG molecule (Figure 1B). In contrast, the LC-cutinase structure was determined as a monomer in the absence of PEG. The high degree of similarity in the structure around the active site between LC-cutinase and *T. alba* cutinase suggests that PEG binds to LC-cutinase, as well. In addition, it has been reported that *T. alba* cutinase is stabilized in the presence of calcium ions.[13,31] To examine whether LC-cutinase is stabilized by PEG and calcium ions, the thermal stability of LC-cutinase was analyzed in the presence of PEG or calcium ions. The thermal denaturation curve of LC-cutinase measured in the presence of 1% PEG and that measured in the presence of 10 mM $CaCl_2$ are shown in Figure 2. The $T_{1/2}$ values of LC-cutinase determined from these curves are summarized in Table 2. The $T_{1/2}$ value of LC-cutinase increases by 8.4 °C in the presence of calcium ions and decreases by 3.0 °C in the presence of PEG, indicating that calcium ions stabilize LC-cutinase and that PEG destabilizes it. LC-cutinase is slightly destabilized in the presence of PEG probably because of a change in protein solvation, as reported for hen egg-white lysozyme.[32]

To analyze the stabilizing effect of calcium ions in a more quantitative way, the thermal stability of LC-cutinase was analyzed in the presence of various concentrations of $CaCl_2$. The thermal denaturation curves of LC-cutinase were shifted parallel to that in the absence of calcium ions, such that the $T_{1/2}$ value increases as the $CaCl_2$ concentration increases up to 98 °C (data not shown). The dependence of the $\Delta T_{1/2}$ value, which represents the difference between the $T_{1/2}$ values of LC-cutinase in the presence and absence of calcium ions, on the $CaCl_2$ concentration is shown in Figure 3. From the data shown

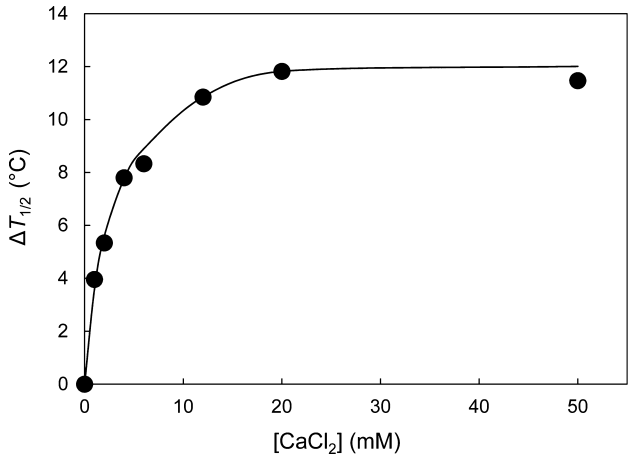

Figure 3. Plot of $\Delta T_{1/2}$ as a function of the concentration of added $CaCl_2$. The $T_{1/2}$ values were determined from the thermal denaturation curves of LC-cutinase obtained in the presence and absence of various concentrations of $CaCl_2$, as described in Materials and Methods. $\Delta T_{1/2}$ represents the difference in the $T_{1/2}$ values of LC-cutinase in the presence and absence of calcium ions (the $T_{1/2}$ of LC-cutinase in the presence of $CaCl_2$ minus the $T_{1/2}$ of LC-cutinase in the absence of $CaCl_2$). The line represents the optimal fit to the data.

in this figure, the number and the dissociation constant of the calcium ion(s) were determined to be 1.05 ± 0.03 and 2.50 ± 0.31 mM, respectively, by Scatchard analysis,[33] on the assumption that LC-cutinase exists in equilibrium between calcium-bound and calcium-free forms and the fraction of the calcium-bound form increases as the $CaCl_2$ concentration increases. These results suggest that LC-cutinase is stabilized by a single calcium ion and its dissociation constant is 2.50 mM. This dissociation constant is apparently lower than those for binding of calcium ions to *T. alba* cutinase, because a considerably high concentration of calcium ions (200 mM) is required to maximize the stability of *T. alba* cutinase.[13] *T. alba* cutinase is stabilized by approximately 13 °C in the presence of 200 mM $CaCl_2$.[31]

The structures of LC-cutinase and *T. alba* cutinase deposited in the PDB (entries 4EB0 and 3VIS, respectively) do not

dx.doi.org/10.1021/bi401561p | *Biochemistry* 2014, 53, 1858−1869

contain any calcium ions, because these structures were determined in the absence of calcium ions. The structure of *T. alba* cutinase in a calcium-bound form has recently been determined by using the crystals soaked in a $CaCl_2$ solution.[31] According to this structure, two calcium ions bind to the protein. One of these calcium ions is apparently coordinated with Asp243, Asp290, and Glu292, while the other is apparently coordinated with Asp236 and the C-terminal carboxyl group. Asp243 and Asp290 are conserved as Asp238 and Asp283, respectively, in LC-cutinase (Figure S1 of the Supporting Information). However, these residues are not located at a distance that allows coordination of the calcium ion. The distance between these residues is 11.1 Å, whereas that between Asp243 and Asp290 of *T. alba* cutinase is 6.2 Å. In addition, Glu292 is replaced with Arg (Arg286) in LC-cutinase (Figure S1 of the Supporting Information). Likewise, Asp236 is replaced with Pro (Pro231) in LC-cutinase (Figure S1 of the Supporting Information). These results suggest that a single calcium ion does not bind to the site, which corresponds to either of the calcium binding sites of *T. alba* cutinase, but binds to the unique site in LC-cutinase. Further structural and mutational studies will be required to identify this site.

Equilibrium Unfolding of LC-Cutinase in GdnHCl. Equilibrium unfolding of LC-cutinase in GdnHCl was analyzed at 30 °C by monitoring the CD values at 222 nm. GdnHCl-induced unfolding of this protein was fully reversible and followed a two-state mechanism under the condition examined. The protein unfolded by GdnHCl was fully refolded by removal of GdnHCl by dialysis (data not shown). The GdnHCl-induced unfolding curve of LC-cutinase is shown in Figure 4. To obtain this curve, the protein was incubated in the presence of various concentrations of GdnHCl for 2 days. This curve was not obtained when the incubation time was short. For example, LC-cutinase was not unfolded when it was incubated in the presence of 6 M GdnHCl for 30 min and was not fully unfolded when it was incubated in the presence of 5 M GdnHCl for 18 h (Figure 4). The GdnHCl-induced unfolding curve of LC-cutinase obtained after a 2 day incubation was not significantly changed upon further incubation. This result suggests that unfolding of LC-cutinases is slow, and it takes at least 2 days for the unfolding reaction of LC-cutinase to reach equilibrium. The C_m and $\Delta G(H_2O)$ values of LC-cutinase were 4.02 M and 41.8 kJ mol^{-1}, respectively (Table 3).

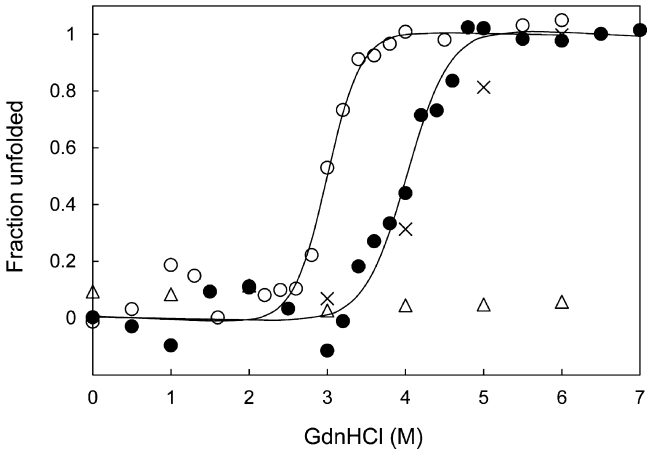

Figure 4. GdnHCl-induced unfolding curves of LC-cutinase and C275/292A-cutinase at 30 °C. The apparent fraction of unfolded protein is shown as a function of GdnHCl concentration. LC-cutinase was incubated for 48 h (●), 18 h (×), and 30 min (△) at pH 8.0 and 30 °C prior to the measurement of the CD value at 222 nm. C275/292A-cutinase (○) was incubated under the same condition for 24 h prior to the measurement of the CD value at 222 nm. The lines represent the fits to eq 1.

The C_m values of *F. solani pisi* and *H. insolens* cutinases for GdnHCl-induced unfolding have been reported to be 1.35 and 1.94 M, respectively.[18] These values are considerably lower than that of LC-cutinase, suggesting that LC-cutinase is more stable than these fungal cutinases. However, the $\Delta G(H_2O)$ values of these proteins (47−49 kJ mol^{-1}) are rather higher than that of LC-cutinase because of their high *m* values.

GdnHCl-Induced Unfolding Kinetics of LC-Cutinase. The equilibrium studies of GdnHCl-induced unfolding of LC-cutinases suggest that LC-cutinase unfolds very slowly. To determine the unfolding rate of this protein, GdnHCl-induced unfolding kinetics of this protein were analyzed at 50 °C by monitoring the CD values at 222 nm. These analyses were performed at 50 °C, instead of 30 °C, because unfolding of this protein was too slow to be completed within several hours at 30 °C. All unfolding reactions gave monophasic kinetics. Typical kinetic traces for unfolding of LC-cutinase are shown in Figure 5A. The dependence of the logarithm of the apparent rate constant of unfolding, k_{app}, on the GdnHCl concentration is shown in Figure 5B. From this dependence, the rate constant of unfolding of LC-cutinase in the absence of GdnHCl, $k_u(H_2O)$, was calculated to be 3.28×10^{-6} s^{-1} (Table 3).

The unfolding rates of *F. solani pisi* and *H. insolens* cutinase have been reported to be 2.57 and 0.829 s^{-1}, respectively, at 25 °C.[18] These unfolding rates are at least 6 orders of magnitude higher than that of LC-cutinase, indicating that LC-cutinase is a kinetically robust protein. However, LC-cutinase is still less stable than hyperthermophilic archaeal proteins, which are characterized by an extremely slow unfolding rate.[34] For example, the unfolding rate of LC-cutinase is 2 orders of magnitude higher than that of RNase H2 from hyperthermophilic archaeon *Thermococcus kodakarensis* (5.0×10^{-8} s^{-1} at 50 °C).[26]

The refolding experiments were also performed at 30 °C using LC-cutinase fully unfolded in the presence of 5 M GdnHCl. However, this protein was not refolded by reducing the GdnHCl concentration by dilution, and therefore, the kinetic refolding curves of this protein were not obtained (data not shown). This protein was kept soluble upon dilution but was kept unfolded even after a 5 day incubation at 30 °C. In contrast, this protein was fully refolded when the GdnHCl concentration was reduced by dialysis, instead of dilution, suggesting that this protein is refolded only when the GdnHCl concentration is gradually decreased. This protein may be trapped in an unfolded state when the GdnHCl concentration is rapidly decreased.

Kinetic Parameters for the Activity of LC-Cutinase at Various Temperatures. The temperature dependence of the activity of LC-cutinase toward *p*NP-butyrate indicated that LC-cutinase exhibited the highest activity at 50 °C (Figure 6A). This result is consistent with that previously reported.[17] However, LC-cutinase is not thermally denatured up to 75 °C (Figure 2). This means that the activity of LC-cutinase decreases as the temperature increases beyond 50 °C, before the protein is thermally denatured. To examine whether a decrease in the activity at these temperatures is due to a decrease in the substrate binding affinity or turnover number of

Table 3. Thermodynamic Parameters at 30 °C and Kinetic Parameters at 50 °C for GdnHCl-Induced Unfolding of LC- and C275/292A-Cutinases

protein	C_m (M)	m_{av}[a] (kJ mol^{-1} M^{-1})	$\Delta G(H_2O)$ (kJ mol^{-1})	$\Delta\Delta G(H_2O)$[b] (kJ mol^{-1})	$k_u(H_2O)$ (s^{-1})
LC-cutinase	4.02 ± 0.03	10.4	41.8 ± 0.3	–	(3.28 ± 0.60) × 10^{-6}
C275/292A-cutinase	3.00 ± 0.10	10.4	31.2 ± 1.0	−10.6	(1.83 ± 0.14) × 10^{-5}

[a]The average of the m values of LC-cutinase (9.2 ± 1.4 kJ mol^{-1} M^{-1}) and C275/292A-cutinase (11.7 ± 1.6 kJ mol^{-1} M^{-1}). [b]$\Delta\Delta G(H_2O)$ = $\Delta G(H_2O)$(C275/292A-cutinase) − $\Delta G(H_2O)$(LC-cutinase).

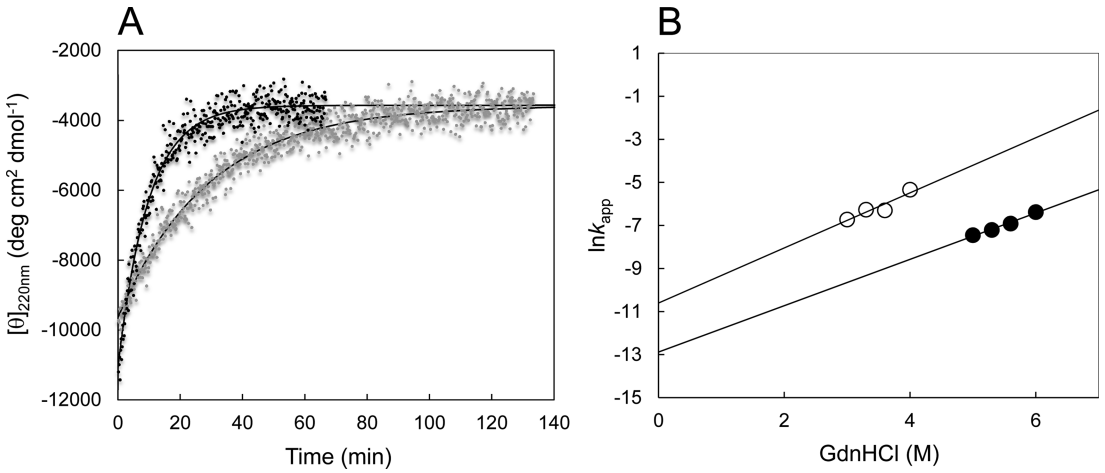

Figure 5. Unfolding kinetics of LC-cutinase and C275/292A-cutinase at 50 °C. (A) Kinetic traces of GdnHCl-induced unfolding of LC-cutinase to final GdnHCl concentrations of 5.0 M (gray scatter) and 6.0 M (black scatter) are shown. The lines represent the fits of eq 3. (B) GdnHCl concentration dependence of the apparent rate constant (k_{app}) of unfolding kinetics of LC-cutinase (●) and C275/292A-cutinase (○). The lines represent the fits of eq 4.

this protein, the kinetic parameters for the activity of LC-cutinase were determined at various temperatures using *p*NP-butyrate as a substrate. At any substrate concentration and temperature examined, the amount of the product increases in proportion to the incubation time for at least 10 min (data not shown). The K_m values of LC-cutinase determined at 30, 50, and 70 °C were similar with one another (0.21−0.24 mM), whereas its k_{cat} values determined at these temperatures varied in proportion to its specific activities (Table 4). These results indicate that a decrease in the activity of LC-cutinase at 60−70 °C as compared to the maximal value is not due to a decrease in the substrate binding affinity but due to a decrease in the turnover number. The steric configurations of the active site residues are probably changed at these temperatures, such that they are not optimal for activity. Thus, the activity of LC-cutinase is reduced at 60−70 °C probably because of a heat-induced local conformational change of the active site. A similar finding that low concentrations of GdnHCl cause local unfolding of the active site region and thereby cause a decrease in enzymatic activity has been reported for *F. solani pisi* cutinase.[18] The optimal temperature for the activity of *T. alba* cutinase, which is identical to that of LC-cutinase (50 °C),[35] is also lower than the stability of the overall structure, but by only 10 °C, suggesting that a heat-induced local conformational change of the active site of *T. alba* cutinase is less significant than that of LC-cutinase.

The K_m and k_{cat} values of other cutinases have been reported to be 1.93 mM and 6.03 s^{-1} for *T. alba* cutinase at 30 °C,[36] 2.10 mM and 30.9 s^{-1} for *T. fusca* cutinase at 25 °C,[37] 0.51 mM and 742 s^{-1} for *T. fusca* cutinase at 60 °C,[38] and 0.27 mM and 837 s^{-1} for *F. solani pisi* cutinase at 40 °C, respectively.[38] The K_m and k_{cat} values of LC-cutinase are 0.22 mM and 232 s^{-1} at 30 °C and 0.21 mM and 343 s^{-1} at 50 °C, respectively (Table 4). These results indicate that both the substrate binding affinity and turnover number of LC-cutinase are considerably higher than those of *T. alba* and *T. fusca* cutinases at 30 °C, whereas they are comparable to those of *T. fusca* and *F. solani pisi* cutinases at 50 °C.

Protection of the Active Site from Heat-Induced Local Conformational Changes by PEG and PET. The finding that LC-cutinase is slightly destabilized in the presence of PEG (Figure 2) suggests that PEG does not bind to the active site of the protein or binding of PEG to the active site does not increase the stability of the overall structure. To examine whether the active site is protected from a heat-induced local conformational change by PEG, the enzymatic activity of LC-cutinase was determined in the presence of 1% PEG 1000 at various temperatures. The temperature dependence of the activity shows that the optimal temperature for activity of LC-cutinase is shifted upward by 10 °C in the presence of PEG (Figure 6B). The specific activities of LC-cutinase determined in the presence of PEG at 10−50 °C are slightly higher than but comparable to those determined in the absence of PEG. To examine whether the specific activity of LC-cutinase increases in the presence of PEG compared to that in the absence of PEG at ≥60 °C due to an increase in the substrate binding affinity or turnover number, the kinetic parameters of LC-cutinase were determined in the presence of 1% PEG at 30, 50, and 70 °C. The kinetic parameters of LC-cutinase determined in the presence of PEG at 30 and 50 °C were comparable to those determined in the absence of PEG at 30 and 50 °C, respectively (Table 4). The K_m value determined in the presence of PEG at 70 °C was also comparable to that determined in the absence of PEG. However, the k_{cat} value of LC-cutinase determined in the presence of PEG at 70 °C is higher than that determined in the absence of PEG by 50%, suggesting that the activity of LC-

dx.doi.org/10.1021/bi401561p | *Biochemistry* 2014, 53, 1858−1869

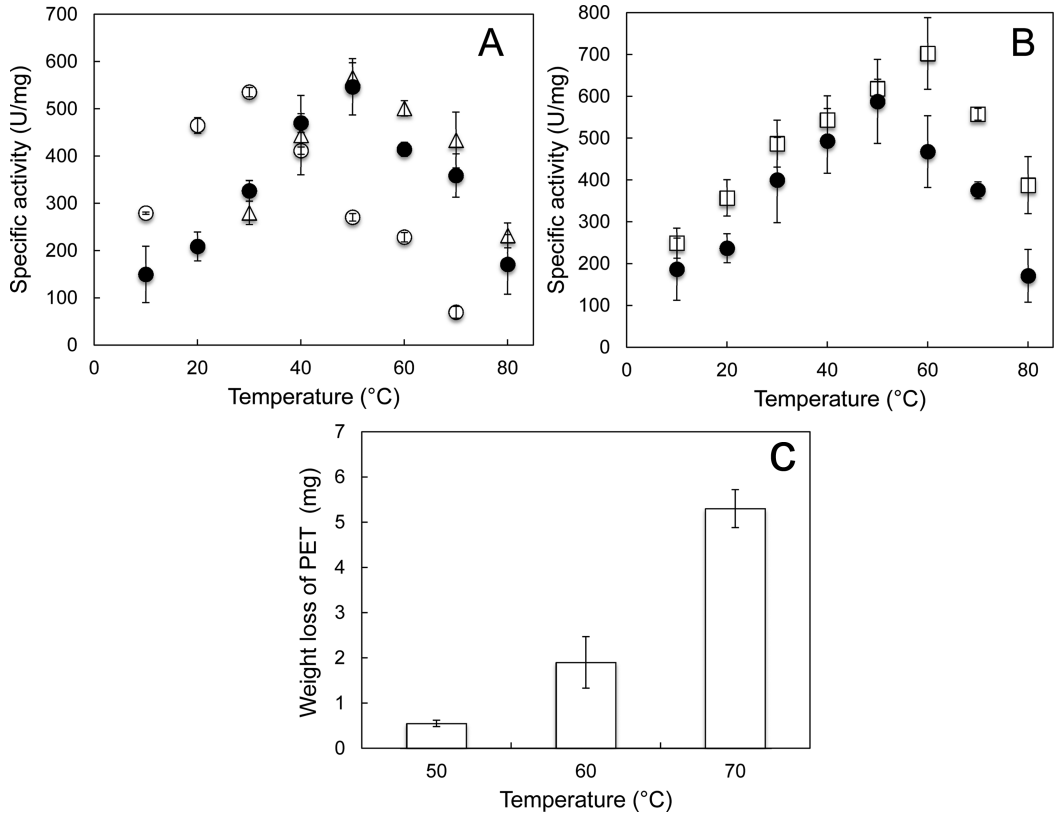

Figure 6. Temperature dependencies of enzymatic activities of LC-cutinase and C275/292A-cutinase. (A) The enzymatic activities of LC-cutinase (●) and C275/292A-cutinase (○) were determined in 10 mM Tris-HCl (pH 8.0) containing 10% (v/v) acetonitrile and 0.5 mM *p*NP-butyrate at the temperatures indicated. The enzymatic activities of LC-cutinase were also determined under the same condition in the presence of 10 mM $CaCl_2$ at the temperatures indicated (△). (B) The enzymatic activities of LC-cutinase determined in 10 mM Tris-HCl (pH 8.0) containing 10% (v/v) acetonitrile, 2 mM *p*NP-butyrate, and 1% PEG1000 at the temperatures indicated (□) are compared with those determined in the absence of PEG1000 (●). (C) The PET-degrading activity of LC-cutinase was determined by incubating a PET film (20−25 mg) with LC-cutinase at pH 8.0 at the temperatures indicated for 24 h and by comparing the weight of a PET film before and after incubation. The weight loss was plotted as a function of temperature. The experiment was always performed in duplicate, and the average values are shown together with the error bars in all panels.

Table 4. Kinetic Parameters of LC-Cutinase and C275/292A-Cutinase[a]

protein	temp (°C)	PEG (%)	K_m (mM)	k_{cat} (s^{-1})	k_{cat}/K_m (s^{-1} mM^{-1})
LC-cutinase	30	0	0.22 ± 0.03	232 ± 20	1050
	30	1	0.27 ± 0.03	278 ± 9	1046
	50	0	0.21 ± 0.00	343 ± 4	1630
	50	1	0.27 ± 0.01	359 ± 22	1311
	70	0	0.24 ± 0.01	213 ± 3	888
	70	1	0.25 ± 0.15	318 ± 46	1295
C275/292A-cutinase	30	0	0.25 ± 0.02	342 ± 25	1370
	50	0	0.18 ± 0.01	196 ± 7	1090
	70	0	0.19 ± 0.02	49 ± 3	258

[a]Hydrolysis of *p*NP-butyrate by the enzyme was conducted at the temperatures indicated under the conditions described in Materials and Methods. Experiments were conducted at least twice, and the average values are shown together with the errors.

cutinase increases in the presence of PEG at ≥60 °C due to an increase in the turnover number. These results suggest that PEG binds to the region near the active site and partially prevents a heat-induced conformational change in the active site, because the optimal temperature for the activity of LC-cutinase in the presence of PEG (60 °C) is still much lower than its denaturation temperature (86.2 °C).

To examine whether the active site of LC-cutinase is protected from a heat-induced local conformational change by a long-chain substrate, as well, the activity of LC-cutinase toward PET was analyzed by measuring the weight loss of a PET film at various temperatures. The activity of LC-cutinase toward PET increased as the temperature increased to 70 °C (Figure 6C), indicating that the optimal temperature for the activity of LC-cutinase toward PET increases by at least 20 °C as compared to that toward *p*NP-butyrate. These results suggest that a heat-induced local conformational change in the active site is well prevented by binding of a long-chain substrate. However, we cannot exclude the possibility that the PET-degrading activity of LC-cutinase decreases at 50 °C as compared to that at 70 °C because of the inertness of the substrate. The activity of LC-cutinase toward PET was not analyzed at temperatures higher than 80 °C, because the surface of a PET film used for the assay became turbid upon incubation at these temperatures and could not be degraded by the enzyme even at 50 °C.

Temperature Dependence of LC-Cutinase Activity in the Presence of Calcium Ions. To examine whether binding of calcium ion affects the enzymatic activity of LC-cutinase, the temperature dependence of the activity of LC-cutinase was analyzed in the presence of 10 mM $CaCl_2$. The optimal temperature for activity was slightly shifted upward by a few degrees Celsius in the presence of calcium ions in proportion to

dx.doi.org/10.1021/bi401561p | *Biochemistry* 2014, 53, 1858−1869

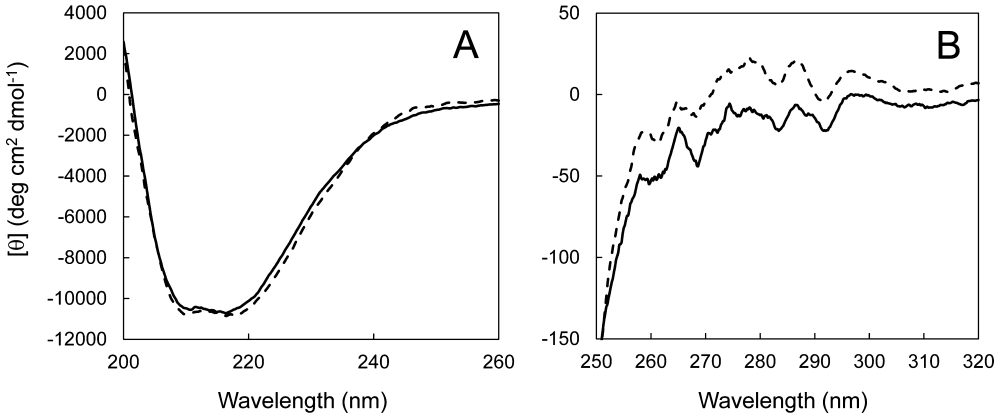

Figure 7. CD spectra of LC-cutinase and C275/292A-cutinase. The far-UV (A) and near-UV (B) CD spectra of LC-cutinase (—) and C275/292A-cutinase (---) are shown. These spectra were measured at 20 °C as described in Materials and Methods.

the stability (Figure 6A). However, the activities of LC-cutinase at 30−50 °C in the presence of calcium ions were comparable to those in the absence of calcium ions (Figure 6A). This result is consistent with the previous result that the enzymatic activity of LC-cutinase is not significantly changed in the presence of either 10 mM $CaCl_2$ or 10 mM EDTA.[17] This result indicates that calcium ion stabilizes the protein without significantly affecting its activity. It has been reported that *T. alba* cutinase does not require calcium ions for activity but requires them for maximal activity.[13] The activity of *T. alba* cutinase decreases by 47% in the presence of 0.5 mM EDTA and increases by 3−4-fold in the presence of 300 mM $CaCl_2$. The effect of calcium ion on the LC-cutinase activity is different from that on the *T. alba* cutinase activity, probably because the calcium binding site of LC-cutinase is different from those of *T. alba* cutinase. The activity of LC-cutinase was not analyzed at >10 mM $CaCl_2$, because its calcium binding site is almost fully saturated with calcium ion in the presence of 10 mM $CaCl_2$ (Figure 3).

Preparation of C275/292A-Cutinase. The single disulfide bond formed between Cys275 and Cys292 of LC-cutinase, which anchors the C-terminus to the central region, is conserved in thermophilic bacterial cutinases but not in fungal cutinases. The disulfide bond is one of the stabilizing factors of the protein. Proteins are usually destabilized by the removal of a native disulfide bond[39−42] and stabilized by introduction of a non-native disulfide bond.[43−47] Therefore, the C-terminal disulfide bond of bacterial cutinase is probably important for protein stability. However, the disulfide bond does not always show a stabilizing effect.[8,48] To examine whether the disulfide bond of LC-cutinase contributes to the thermodynamic and kinetic stability of LC-cutinase, the double-mutant protein C275/292A-cutinase, in which both Cys275 and Cys292 are replaced with Ala, was constructed and purified. The purified recombinant protein, in which a seven-residue peptide is attached to C275/292A-cutinase[36−293], will be simply designated as C275/292A-cutinase hereafter. The production level and purification yield of C275/292A-cutinase were comparable to those of LC-cutinase. The far-UV (Figure 7A) and near-UV (Figure 7B) CD spectra of C275/292A-cutinase were similar to those of LC-cutinase, suggesting that the structure of LC-cutinase is not markedly changed by the mutations.

Thermal Stability of C275/292A-Cutinase. To examine whether removal of the disulfide bond affects the thermal stability of LC-cutinase, the stability of C275/292A-cutinase was analyzed at pH 8.0 as mentioned above for LC-cutinase. The stability of LC- and C275/292A-cutinases was also analyzed in the presence of 10 mM DTT. Thermal denaturation of these proteins was irreversible under the conditions examined. The resultant thermal denaturation curves are shown in Figure 2. The $T_{1/2}$ values determined from these curves are summarized in Table 2. The $T_{1/2}$ value of C275/292A-cutinase measured in the absence of DTT is lower than that of LC-cutinase by 15.6 °C, whereas the $T_{1/2}$ value of LC-cutinase measured in the presence of DTT is lower than that measured in the absence of DTT by 12.3 °C. However, the $T_{1/2}$ value of C275/292A-cutinase measured in the presence of DTT is higher than that measured in the absence of DTT by 2.0 °C, suggesting that the difference between the $T_{1/2}$ values of oxidized and reduced forms of LC-cutinase is 14.3 °C, instead of 12.3 °C. The mechanism by which C275/292A-cutinase is slightly stabilized in the presence of DTT remains to be understood. These results indicate that LC-cutinase is destabilized by approximately 15 °C, regardless of whether the disulfide bond is removed by reduction or by double mutations at Cys275 and Cys292. The $T_{1/2}$ value of LC-cutinase does not significantly decrease further in the presence of higher concentrations of DTT, suggesting that the disulfide bond of LC-cutinase is almost fully reduced in the presence of 10 mM DTT (data not shown).

Equilibrium Unfolding of C275/292A-Cutinase in GdnHCl. To examine whether removal of the disulfide bond affects equilibrium unfolding of LC-cutinase in GdnHCl, GdnHCl-induced unfolding of C275/292A-cutinase was analyzed at 30 °C as mentioned above for LC-cutinase. GdnHCl-induced unfolding of this protein was fully reversible and followed a two-state mechanism. The GdnHCl-induced unfolding curve of C275/292A-cutinase is shown in Figure 4. To obtain this curve, the protein was incubated in the presence of various concentrations of GdnHCl for 1 day, instead of 2 days. This result suggests that C275/292A-cutinase unfolds more rapidly than LC-cutinase, but it still takes at least 1 day for the unfolding reaction of C275/292A-cutinase to reach equilibrium. Thermodynamic parameters for GdnHCl-induced unfolding of C275/292A-cutinase are summarized in Table 3. The C_m and $\Delta G(H_2O)$ values of C275/292A-cutinase are lower than those of LC-cutinase by 1.02 M and 10.6 kJ mol^{-1}, respectively. We used the average of the *m* values of LC- and C275/292A-cutinases for the calculation of the $\Delta G(H_2O)$ values of these proteins. If we use the *m* values of LC- and

dx.doi.org/10.1021/bi401561p | *Biochemistry* 2014, 53, 1858−1869

C275/292A-cutinases, which were determined to be 9.2 and 11.7 kJ mol^{-1} M^{-1}, respectively, for calculation of the $\Delta G(H_2O)$ values, the $\Delta G(H_2O)$ value of C275/292A-cutinase is lower than that of LC-cutinase by only 2.0 kJ mol^{-1}. Despite this observed difference, the results indicate that the thermodynamic stability of LC-cutinase is significantly decreased by removal of the disulfide bond.

The contribution of the disulfide bond to protein stability is presumed to be mainly due to a loss of conformational entropy in the unfolded state.[49] This loss can be estimated using eq 5:

$$\Delta S = -2.1 - \left(\frac{3}{2}\right) R \ln n \quad (5)$$

where R is the gas constant and n is the number of the residues in the loop forming the disulfide bond.[39] Because n is 18 for the disulfide bond of LC-cutinase (Cys275−Cys292), the ΔS value at 30 °C ($T\Delta S$) for this disulfide bond is calculated to be −11.6 kJ mol^{-1}. This means that the difference in the ΔG values ($\Delta\Delta G$) between the proteins with and without a disulfide bond is 11.6 kJ mol^{-1}, if the enthalpy change (ΔH) is negligible. This value is comparable to the $\Delta\Delta G$ value (10.6 kJ mol^{-1}) between LC-cutinase and C275/292A-cutinase determined by the GdnHCl-induced equilibrium unfolding studies.

GdnHCl-Induced Unfolding Kinetics of C275/292A-Cutinase. The equilibrium studies of GdnHCl-induced unfolding of C275/292A-cutinase suggest that the disulfide bond at least partly contributes to the slow unfolding of LC-cutinase. To determine the unfolding rate of C275/292A-cutinase, the GdnHCl-induced unfolding kinetics of this protein were analyzed at 50 °C as mentioned above for LC-cutinase. All unfolding reactions gave monophasic kinetics. Typical kinetic traces for unfolding of C275/292A-cutinase are shown in Figure S2 of the Supporting Information. The dependence of the k_{app} values on the GdnHCl concentration is shown in Figure 5B. From this dependence, the $k_u(H_2O)$ value of C275/292A-cutinase was calculated to be 1.83×10^{-5} s^{-1} (Table 3). Thus, the unfolding rate of C275/292A-cutinase is 1 order of magnitude higher than that of LC-cutinase, indicating that the disulfide bond of LC-cutinase contributes not only to the thermodynamic stability but also to the kinetic stability of the protein.

Temperature Dependence of the Activity of C275/292A-Cutinase. To examine whether removal of the disulfide bond affects the optimal temperature for the activity of LC-cutinase, the temperature dependence of the activity of C275/292A-cutinase was analyzed by using *p*NP-butyrate as a substrate. C275/292A-cutinase exhibited its highest activity at 30 °C (Figure 6A). The activity of C275/292A-cutinase at 30 °C was comparable to that of LC-cutinase at 50 °C. These results indicate that removal of the disulfide bond shifts the optimal temperature for activity of LC-cutinase downward by 20 °C without significantly affecting the maximal activity.

Relationship between the Stability of the Active Site and the Overall Structure. In this study, we showed that the optimal temperature for the activity of LC-cutinase decreases upon removal of the disulfide bond and increases upon binding of a calcium ion to the protein in proportion to the stability of the overall structure. This result suggests that the stability of the local structure around the active site varies in proportion to the stability of the overall structure. A similar relationship between the stability of the active site and overall structure has also been reported for *Bacillus subtilis* esterase and its mutants.[50] However, an inverse relationship between these stabilities is observed for LC-cutinase in the presence of PEG. This result may suggest that PEG stabilizes the overall structure by binding to the region near the active site, but this stabilization effect is canceled by the destabilization effect of PEG for the overall structure. Alternatively, PEG stabilizes the local structure around the active site by binding to this region without significantly affecting the stability of the overall structure. The reason why binding of PEG to the region near the active site stabilizes this region without significantly affecting the stability of the overall structure remains to be understood.

Structural Features of Thermostable LC-Cutinase. LC-cutinase is more stable than *T. alba* cutinase by approximately 26 °C. Proteins are stabilized by a combination of various factors, such as an increased number of ion pairs (ion pair networks),[51] a reduced cavity volume,[52] anchoring of the C-terminal tail,[53] increased interior hydrophobicity,[54] an increased number of proline residues in loop regions,[55] and an increased number of disulfide bonds.[56] Comparison of these factors between LC-cutinase and *T. alba* cutinase indicates that the number of ion pairs and interior hydrophobicity of LC-cutinase are higher than those of *T. alba* cutinase, although the difference is not so significant (Table 5). The number of ion pairs is eight for LC-cutinase and six for *T. alba* cutinase, and only two of them are conserved in these proteins. The ratio of interior apolar residues to total interior residues is 68% for LC-cutinase and 62% for *T. alba* cutinase. In contrast, the number of proline residues in loop regions of LC-cutinase (10) is smaller than that of *T. alba* cutinase (11), and seven of them are conserved in these proteins. Likewise, the disulfide bond of LC-cutinase is conserved in *T. alba* cutinase, and this disulfide bond anchors the C-termini of these proteins to the central regions equally. Furthermore, no clear cavity exists in the LC-cutinase and *T. alba* cutinase structures. These results suggest that the difference in the number of ion pairs and interior hydrophobicity may at least partly account for the difference in stability between LC-cutinase and *T. alba* cutinase.

Table 5. Structural Features of LC-Cutinase and *T. alba* Cutinase

	LC-cutinase	*T. alba* cutinase
no. of amino acids	259	263
T_m (°C)	86.2[a]	60[b]
optimal temp for activity (°C)	50[c]	50[d]
content of the residues (%)		
buried polar	19.4	23.4
buried apolar	40.7	38.3
buried apolar/buried total	67.7	62.1
no. of ion pairs (≤4.0 Å)	8	6
no. of disulfide bonds	1	1
no. of Pro residues in the loop	10	11

[a]$T_{1/2}$ value. [b]Data from ref 31. [c]Data from ref 17. [d]Data from ref 35.

■ ASSOCIATED CONTENT

Supporting Information

Alignment of the amino acid sequences of LC-cutinase (LCC), *T. alba* cutinase (TaC), and *T. fusca* cutinase (TfC) (Figure S1) and unfolding kinetics of C275/292A-cutinase at 50 °C (Figure S2). This material is available free of charge via the Internet at http://pubs.acs.org.

Accession Codes

Coordinates for LC-cutinase were deposited as Protein Data Bank entry 4EB0.

AUTHOR INFORMATION

Corresponding Author

*Telephone and fax: +81-6-6879-7938. E-mail: kanaya@mls.eng.osaka-u.ac.jp.

Funding

This work was supported in part by Grant 24380055 from the Ministry of Education, Culture, Sports, Science, and Technology of Japan and the JSPS Japanese-German Graduate Externship. D.-J.Y. was financially supported by Korea Basic Science Institute Grant T33415.

Notes

The authors declare no competing financial interest.

ACKNOWLEDGMENTS

The synchrotron radiation experiments were performed at Osaka University beamline BL44XU at SPring-8 with the approval of the Japan Synchrotron Radiation Research Institute (JASRI) (Proposal 2011B6612). We thank Dr. K. Takano (Graduate School of Life and Environmental Sciences, Kyoto Prefectural University, Kyoto, Japan) for helpful discussions.

ABBREVIATIONS

LC-cutinase, metagenome-derived cutinase from leaf-branch compost; C275/292A-cutinase, LC-cutinase derivative with mutations of Cys275 and Cys292 to Ala; *p*NP-butyrate, *p*-nitrophenyl butyrate; PEG, polyethylene glycol; PET, polyethylene terephthalate; GdnHCl, guanidine hydrochloride; CD, circular dichroism; DTT, dithiothreitol; PDB, Protein Data Bank; rmsd, root-mean-square deviation.

REFERENCES

(1) Purdy, R. E., and Kolattukudy, P. E. (1975) Hydrolysis of plant cuticle by plant pathogens. Purification, amino acid composition, and molecular weight of two isozymes of cutinase and a nonspecific esterase from *Fusarium solani f. pisi*. *Biochemistry 14*, 2824−2831.

(2) Carvalho, C. M. L., Aires-Barros, M. R., and Cabral, J. M. S. (1998) Cutinase structure, function and biocatalytic applications. *Electron. J. Biotechnol. 1*, 160−173.

(3) Longhi, S., and Cambillau, C. (1999) Structure-activity of cutinase, a small lipolytic enzyme. *Biochim. Biophys. Acta 1441*, 185−196.

(4) Dutta, K., Sen, S., and Veeranki, V. D. (2009) Production, characterization and applications of microbial cutinases. *Process Biochem. 44*, 127−134.

(5) Chen, S., Su, L., Chen, J., and Wu, J. (2013) Cutinase: Characteristics, preparation, and application. *Biotechnol. Adv. 31*, 1754−1767.

(6) Nyon, M. P., Rice, D. W., Berrisford, J. M., Hounslow, A. M., Moir, A. J. G., Huang, H., Nathan, S., Mahadi, N. M., Bakar, F. D. A., and Craven, C. J. (2009) Catalysis by *Glomerella cingulata* cutinase requires conformational cycling between the active and inactive states of its catalytic triad. *J. Mol. Biol. 385*, 226−235.

(7) Liu, Z., Gosser, Y., Baker, P. J., Ravee, Y., Lu, Z., Alemu, G., Li, H., Butterfoss, G. L., Kong, X.-P., Gross, R., and Montclare, J. K. (2009) Structural and functional studies of *Aspergillus oryzae* cutinase: Enhanced thermostability and hydrolytic activity of synthetic ester and polyester degradation. *J. Am. Chem. Soc. 131*, 15711−15716.

(8) Fernandes, A. T., Pereira, M. M., Silva, C. S., Lindley, P. F., Bento, I., Melo, E. P., and Martins, L. O. (2011) The removal of a disulfide bridge in CotA-laccase changes the slower motion dynamics involved in copper binding but has no effect on the thermodynamic stability. *JBIC, J. Biol. Inorg. Chem. 16*, 641−651.

(9) Kodama, Y., Masaki, K., Kondo, H., Suzuki, M., Tsuda, S., Nagura, T., Shimba, N., Suzuki, E., and Iefuji, H. (2009) Crystal structure and enhanced activity of a cutinase-like enzyme from *Cryptococcus sp.* strain S-2. *Proteins 77*, 710−717.

(10) Pio, T. F., and Macedo, G. A. (2009) Cutinases: Properties and industrial applications. *Adv. Appl. Microbiol. 66*, 77−95.

(11) Araújo, R., Silva, C., O'Neill, A., Micaelo, N., Guebitz, G., Soares, C. M., Casal, M., and Cavaco-Paulo, A. (2007) Tailoring cutinase activity towards polyethylene terephthalate and polyamide 6,6 fibers. *J. Biotechnol. 128*, 849−857.

(12) Silva, C., Da, S., Silva, N., Matamá, T., Araújo, R., Martins, M., Chen, S., Chen, J., Wu, J., Casal, M., and Cavaco-Paulo, A. (2011) Engineered *Thermobifida fusca* cutinase with increased activity on polyester substrates. *Biotechnol. J. 6*, 1230−1239.

(13) Thumarat, U., Nakamura, R., Kawabata, T., Suzuki, H., and Kawai, F. (2012) Biochemical and genetic analysis of a cutinase-type polyesterase from a thermophilic *Thermobifida alba* AHK119. *Appl. Microbiol. Biotechnol. 95*, 419−340.

(14) Herrero Acero, E., Ribitsch, D., Dellacher, A., Zitzenbacher, S., Marold, A., Steinkellner, G., Gruber, K., Schwab, H., and Guebitz, G. M. (2013) Surface engineering of a cutinase from *Thermobifida cellulosilytica* for improved polyester hydrolysis. *Biotechnol. Bioeng. 110*, 2581−2590.

(15) Zhang, Y., Wang, L., Chen, J., and Wu, J. (2013) Enhanced activity toward PET by site-directed mutagenesis of *Thermobifida fusca* cutinase-CBM fusion protein. *Carbohydr. Polym. 97*, 124−129.

(16) Ribitsch, D., Yebra, A. O., Zitzenbacher, S., Wu, J., Nowitsch, S., Steinkellner, G., Greimel, K., Doliska, A., Oberdorfer, G., Gruber, C. C., Gruber, K., Schwab, H., Stana-Kleinschek, K., Acero, E. H., and Guebitz, G. M. (2013) Fusion of binding domains to *Thermobifida cellulosilytica* cutinase to tune sorption characteristics and enhancing PET hydrolysis. *Biomacromolecules 14*, 1769−1776.

(17) Sulaiman, S., Yamato, S., Kanaya, E., Kim, J.-J., Koga, Y., Takano, K., and Kanaya, S. (2012) Isolation of a novel cutinase homolog with polyethylene terephthalate-degrading activity from leaf-branch compost by using a metagenomic approach. *Appl. Environ. Microbiol. 78*, 1556−1562.

(18) Ternström, T., Svendsen, A., Akke, M., and Adlercreutz, P. (2005) Unfolding and inactivation of cutinases by AOT and guanidine hydrochloride. *Biochim. Biophys. Acta 1748*, 74−83.

(19) Goodwin, T. W., and Morton, R. A. (1946) The spectrophotometric determination of tyrosine and tryptophan in proteins. *Biochem. J. 40*, 628−632.

(20) Otwinowski, Z., and Minor, W. (1997) Processing of X-ray diffraction data collected in oscillation mode. *Methods Enzymol. 276*, 307−326.

(21) Vagin, A., and Teplyakov, A. (1997) MOLREP: An Automated Program for Molecular Replacement. *J. Appl. Crystallogr. 30*, 1022−1025.

(22) Collaborative Computational Project, Number 4 (1994) The CCP4 suite: Programs for protein crystallography. *Acta Crystallogr. D50*, 760−763.

(23) Langer, G., Cohen, S. X., Lamzin, V. S., and Perrakis, A. (2008) Automated macromolecular model building for X-ray crystallography using ARP/wARP version 7. *Nat. Protoc. 3*, 1171−1179.

(24) Murshudov, G. N., Vagin, A. A., and Dodson, E. J. (1997) Refinement of macromolecular structures by the maximum-likelihood method. *Acta Crystallogr. D53*, 240−255.

(25) Emsley, P., and Cowtan, K. (2004) Coot: Model-building tools for molecular graphics. *Acta Crystallogr. D60*, 2126−2132.

(26) Mukaiyama, A., Takano, K., Haruki, M., Morikawa, M., and Kanaya, S. (2004) Kinetically robust monomeric protein from a hyperthermophile. *Biochemistry 43*, 13859−13866.

(27) Pace, C. N. (1990) Measuring and increasing protein stability. *Trends Biotechnol. 8*, 93−98.

(28) Kitadokoro, K., Thumarat, U., Nakamura, R., Nishimura, K., Karatani, H., Suzuki, H., and Kawai, F. (2012) Crystal structure of

cutinase Est119 from *Thermobifida alba* AHK119 that can degrade modified polyethylene terephthalate at 1.76 Å resolution. *Polym. Degrad. Stab. 97*, 771−775.
(29) Wei, Y., Swenson, L., Castro, C., Derewenda, U., Minor, W., Arai, H., Aoki, J., Inoue, K., Servin-Gonzalez, L., and Derewenda, Z. S. (1998) Structure of a microbial homologue of mammalian platelet-activating factor acetylhydrolases: *Streptomyces exfoliatus* lipase at 1.9 Å resolution. *Structure 6*, 511−519.
(30) Ollis, D. L., Cheah, E., Cygler, M., Dijkstra, B., Frolow, F., Franken, S. M., Harel, M., Remington, S. J., Silman, I., and Schrag, J. (1992) The α /β hydrolase fold. *Protein Eng. 5*, 197−211.
(31) Kawai, F., Thumarat, U., Kitadokoro, K., Waku, T., Tada, T., Tanaka, N., and Kawabata, T. (2013) Comparison of polyester-degrading cutinases from genus *Thermobifida*. In *Green Polymer Chemistry: Biocatalysis and Materials II* (Cheng, H. N., Gross, R. A., and Smith, P. B., Eds.) pp 111−120, ACS Symposium Series 1144, American Chemical Society, Washington, DC.
(32) Zielenkiewicz, W., Swierzewski, R., Attanasio, F., and Rialdi, G. (2006) Thermochemical, volumetric and spectroscopic properties of lysozyme−poly(ethylene) glycol system. *J. Therm. Anal. Calorim. 83*, 587−595.
(33) Fletcher, J. E., Spector, A. A., and Ashbrook, J. D. (1970) Analysis of macromolecule−ligand binding by determination of stepwise equilibrium constants. *Biochemistry 9*, 4580−4587.
(34) Okada, J., Okamoto, T., Mukaiyama, A., Tadokoro, T., You, D.-J., Chon, H., Koga, Y., Takano, K., and Kanaya, S. (2010) Evolution and thermodynamics of the slow unfolding of hyperstable monomeric proteins. *BMC Evol. Biol. 10*, 207.
(35) Hu, X., Thumarat, U., Zhang, X., Tang, M., and Kawai, F. (2010) Diversity of polyester-degrading bacteria in compost and molecular analysis of a thermoactive esterase from *Thermobifida alba* AHK119. *Appl. Microbiol. Biotechnol. 87*, 771−779.
(36) Ribitsch, D., Acero, E. H., Greimel, K., Eiteljoerg, I., Trotscha, E., Freddi, G., Schwab, H., and Guebitz, G. M. (2012) Characterization of a new cutinase from *Thermobifida alba* for PET-surface hydrolysis. *Biocatal. Biotransform. 30*, 2−9.
(37) Herrero Acero, E., Ribitsch, D., Steinkellner, G., Gruber, K., Greimel, K., Eiteljoerg, I., Trotscha, E., Wei, R., Zimmermann, W., Zinn, M., Cavaco-Paulo, A., Freddi, G., Schwab, H., and Guebitz, G. (2011) Enzymatic Surface Hydrolysis of PET: Effect of Structural Diversity on Kinetic Properties of Cutinases from *Thermobifida*. *Macromolecules 44*, 4632−4640.
(38) Chen, S., Su, L., Billig, S., Zimmermann, W., Chen, J., and Wu, J. (2010) Biochemical characterization of the cutinases from *Thermobifida fusca*. *J. Mol. Catal. B: Enzym. 63*, 121−127.
(39) Pace, C. N., Grimsley, G. R., Thomson, J. A., and Barnett, B. J. (1988) Conformational stability and activity of ribonuclease T1 with zero, one, and two intact disulfide bonds. *J. Biol. Chem. 263*, 11820−11825.
(40) Piatek, R., Bruździak, P., Wojciechowski, M., Zalewska-Piatek, B., and Kur, J. (2010) The noncanonical disulfide bond as the important stabilizing element of the immunoglobulin fold of the Dr fimbrial DraE subunit. *Biochemistry 49*, 1460−1468.
(41) Schulenburg, C., Weininger, U., Neumann, P., Meiselbach, H., Stubbs, M. T., Sticht, H., Balbach, J., Ulbrich-Hofmann, R., and Arnold, U. (2010) Impact of the C-terminal disulfide bond on the folding and stability of onconase. *ChemBioChem 11*, 978−986.
(42) Mason, J. M., Bendall, D. S., Howe, C. J., and Worrall, J. A. R. (2012) The role of a disulfide bridge in the stability and folding kinetics of *Arabidopsis thaliana* cytochrome c6A. *Biochim. Biophys. Acta 1824*, 311−318.
(43) Matsumura, M., Becktel, W. J., Levitt, M., and Matthews, B. W. (1989) Stabilization of phage T4 lysozyme by engineered disulfide bonds. *Proc. Natl. Acad. Sci. U.S.A. 86*, 6562−6566.
(44) Kanaya, S., Katsuda-Nakai, C., and Ikehara, M. (1991) Importance of the positive charge cluster in *Escherichia coli* ribonuclease HI for the effective binding of the substrate. *J. Biol. Chem. 266*, 11621−11627.
(45) Boone, C. D., Habibzadegan, A., Tu, C., Silverman, D. N., and McKenna, R. (2013) Structural and catalytic characterization of a thermally stable and acid-stable variant of human carbonic anhydrase II containing an engineered disulfide bond. *Acta Crystallogr. D69*, 1414−1422.
(46) Vinther, T. N., Norrman, M., Ribel, U., Huus, K., Schlein, M., Steensgaard, D. B., Pedersen, T. Å., Pettersson, I., Ludvigsen, S., Kjeldsen, T., Jensen, K. J., and Hubálek, F. (2013) Insulin analog with additional disulfide bond has increased stability and preserved activity. *Protein Sci. 22*, 296−305.
(47) Wozniak-Knopp, G., and Rüker, F. (2012) A C-terminal interdomain disulfide bond significantly stabilizes the Fc fragment of IgG. *Arch. Biochem. Biophys. 526*, 181−187.
(48) Schmidt, B., Ho, L., and Hogg, P. J. (2006) Allosteric disulfide bonds. *Biochemistry 45*, 7429−7433.
(49) McAuley, A., Jacob, J., Kolvenbach, C. G., Westland, K., Lee, H. J., Brych, S. R., Rehder, D., Kleemann, G. R., Brems, D. N., and Matsumura, M. (2008) Contributions of a disulfide bond to the structure, stability, and dimerization of human IgG1 antibody C_H3 domain. *Protein Sci. 17*, 95−106.
(50) Giver, L., Gershenson, A., Freskgard, P.-O., and Arnold, F. H. (1998) Directed evolution of a thermostable esterase. *Proc. Natl. Acad. Sci. U.S.A. 95*, 12809−12813.
(51) Karshikoff, A., and Ladenstein, R. (2001) Ion pairs and the thermotolerance of proteins from hyperthermophiles: A "traffic rule" for hot roads. *Trends Biochem. Sci. 26*, 550−556.
(52) Nguyen, T.-N., Angkawidjaja, C., Kanaya, E., Koga, Y., Takano, K., and Kanaya, S. (2012) Activity, stability, and structure of metagenome-derived LC11-RNase H1, a homolog of *Sulfolobus tokodaii* RNase H1. *Protein Sci. 21*, 553−561.
(53) You, D.-J., Chon, H., Koga, Y., Takano, K., and Kanaya, S. (2007) Crystal structure of type 1 ribonuclease H from hyperthermophilic archaeon *Sulfolobus tokodaii*: Role of arginine 118 and C-terminal anchoring. *Biochemistry 46*, 11494−11503.
(54) Pace, C. N., Fu, H., Fryar, K. L., Landua, J., Trevino, S. R., Shirley, B. A., Hendricks, M. M., Iimura, S., Gajiwala, K., Scholtz, J. M., and Grimsley, G. R. (2011) Contribution of hydrophobic interactions to protein stability. *J. Mol. Biol. 408*, 514−528.
(55) Watanabe, K., Chishiro, K., Kitamura, K., and Suzuki, Y. (1991) Proline residues responsible for thermostability occur with high frequency in the loop regions of an extremely thermostable oligo-1,6-glucosidase from *Bacillus thermoglucosidasius* KP1006. *J. Biol. Chem. 266*, 24287−24294.
(56) Boutz, D. R., Cascio, D., Whitelegge, J., Perry, L. J., and Yeates, T. O. (2007) Discovery of a thermophilic protein complex stabilized by topologically interlinked chains. *J. Mol. Biol. 368*, 1332−1344.